Clay Minerals (1999) **34**, 291–299

Distribution of manganese in synthetic goethite

U. G. GASSER, R. NÜESCH*, M. J. SINGER† AND E. JEANROY‡

*College of Engineering, Im Grüntal, CH 8820 Wädenswil, *Department of Materials, Institute of Polymers, ETH, CH 8092 Zürich, Switzerland, † Department of Land, Air and Water Resources, University of California, Davis, CA 95616-8627 USA, and ‡Centre de Pédologie Biologique, U.P.R. 6831 du CNRS, associée à l'Université Henri Poincaré, BP 5, F 54501 Vandœuvre-lès-Nancy, France*

(*Received 21 July 1997; revised 21 May 1998*)

ABSTRACT: A series of Mn-goethites was synthesized at highly alkaline conditions. The samples were aged for 15 days at a final [KOH] of 0.3 M. Products were washed free from non-goethite phases using 3 M H_2SO_4. The bulk mineralogy of the samples was determined by X-ray diffraction and verified on selected individual crystals by electron diffraction. The samples had a relatively low magnetic susceptibility ($300 \leqslant MS \leqslant 400 \times 10^{-9}$ m^3/kg). As revealed by total acid dissolution, the Mn mole fraction X_{Mn} ranged from zero to 0.125. Five samples (X_{Mn}: 0.025, 0.050, 0.077, 0.099, 0.125) were selected to investigate the variability of the X_{Mn} value in single goethite needles (crystals) by analytical electron microscopy (AEM) using rastered and spot analyses. Linear regressions of both as a function of total Mn yielded unit slopes and zero intercepts, indicating that acid dissolution gave the same results as AEM. Spot AEM, however, revealed significant variation of Mn distribution within individual crystals which argues in favour of Mn zoning in goethite. Inhomogeneous transformation of ferrihydrite to goethite may partly explain the Mn zoning.

Iron oxides (Fe oxides) such as goethite (α-FeOOH) and hematite (α-Fe_2O_3) are commonly encountered weathering products at the surface of the earth. In the environment, Fe oxides are reactive substances. They have a high potential to adsorb or incorporate non-iron elements (Schwertmann & Taylor, 1989) such as metal cations (e.g. Al^{3+}, Cr^{3+} and Ni^{2+}), metal anions (e.g. MoO_4^{2-}) and non-metal anions (e.g. phosphate, orthosilicate, selenite and organic matter). Consequently, Fe oxides may control the availability of environmentally important substances such as plant nutrients or toxicants and this is why they have attracted the interest of researchers from many fields of science including agronomy, chemistry, environmental engineering, forestry, geology and soil science.

In nature, Fe oxides such as goethite are generally not pure, but in addition to Fe, contain other cations in their structure, Al^{3+} being the most prominent. Synthetic goethites may also incorporate other metal cations (e.g. Al, Cd, Co, Cr, Cu, Mn, Ni, Pb, V and Zn; Gerth, 1990; Schulze, 1982; Schwertmann *et al*., 1989; Schwertmann & Pfab, 1994; Stiers & Schwertmann, 1985). Generally, X-ray diffraction (XRD) is used to verify the incorporation (except in the case of V^{3+}; Schwertmann & Pfab, 1994).

In pure goethite, Fe is present in its trivalent form. The ionic radius of Fe(III) is 64.5 pm (Shannon, 1976). Most other cations have different ionic radii, which generally leads to a systematic change of one or more unit-cell edge lengths. Other physical and chemical properties such as dehydroxylation temperature, infrared band positions, colour and dissolution rates (both in acid and reductive environments) may change with increasing mole fraction of the substituting cation (Gasser *et al*., 1996; Schwertmann, 1984; Torrent *et al*., 1987; Vempati *et al*., 1995).

In contrast to natural samples, the incorporation of Mn into the structure of synthetic goethite is well established. The ionic radius of Mn(III) is also 64.5 pm (Shannon, 1976). If Mn substitution (X_{Mn} = Mn/(Mn+Fe) [mol mol^{-1}]) exceeds ~0.06 mol

mol^{-1}, other phases such as hausmannite, hematite or jacobsite may be present, (Cornell & Giovanoli, 1987; Ebinger & Schulze, 1989, 1990; Stiers & Schwertmann, 1985; Vempati *et al*., 1995), some of which show a relatively high magnetic susceptibility. Although Mn-goethite syntheses generally start from an Mn(II) system (e.g. $Mn(NO_3)_2$), Mn is considered to be incorporated in its trivalent form (Cornell & Giovanoli, 1987; Gerth, 1990; Stiers & Schwertmann, 1985; A. Scheinost, pers. comm.). Oxidation of Mn is, therefore, required. Adsorption of $Mn(II)_{aq}$ onto minerals including Fe oxides is effectively promoting its oxidation (Junta & Hochella, 1994, and references therein).

Generally, substituted goethites are believed to have a uniform distribution of other cations within a given sample. A natural hematite from Brazil, synthetically enriched in Al (mole fraction X_{Al} = 0.022(4) mol mol^{-1}) had a coefficient of variation (CV) of ~0.2 for the Al substitution (Gharibi *et al*., 1990; no explicit statement of method used). An energy dispersive analysis X-ray (EDAX) study on synthetic Co-goethite indicated that the CV value for the Co mole fraction, X_{Co} may be as high as 0.25 (sample S4: X_{Co} = 0.055(14) mol mol^{-1}; Gasser *et al*., 1996). The question arises whether variations of the mole fraction X (i.e. zoning) in substituted Fe oxides are common or not.

Zoning is a well known feature in geology, mineralogy and crystallography and occurs, e.g. as a result of olivine crystallization by cooling of a Mg-Fe-melt (e.g. Bloss, 1971; Rösler, 1983). It is expressed as a concentric chemical gradient from the centre of a mineral towards its surface. Although zoning of chemical composition is commonly encountered in silicate minerals (e.g. amphiboles, feldspars, garnets, phyllosilicates and pyroxenes), it may occur in any mineral that has a changing solution chemistry during the process of crystallization (e.g. Zoltai & Stout, 1984). Because changes of solution chemistry with time are common in many soils, chemical zoning is also feasible in natural Fe oxides.

The goal of this study was to quantify Mn substitution in synthetic goethites and its variability in a representative selection of samples.

MATERIALS AND METHODS

Goethite preparation

A series of Mn-substituted goethites (M1 to M8) was prepared, starting from a nitrate solution of Fe(III) and Mn(II). This synthesis followed a procedure modified from Schwertmann & Cornell (1991). In a 250 ml polypropylene beaker, 100 ml of 1 M $Fe(NO_3)_3$ was mixed with X ml of 0.5 M $Mn(NO_3)_2$ where X = 0, 1, 5.1, 10.5, 16.2, 22.2 and twice 28.6. The resulting solutions had Mn mole fractions (X_{Mn} = Mn/[Mn+Fe]) of 0.000, 0.005, 0.025, 0.050, 0.075, 0.100 and twice 0.125, respectively. The solutions were then transferred to two-litre polyethylene bottles and Y g of 5 M KOH were added where Y = 214.4, 214.7, 216.2, 218.1, 220.2, 222.3 and twice 224.6. Distilled water was added to obtain a final suspension volume of 2 l and a KOH concentration of 0.3 M. The suspensions were aged for 15 consecutive days at 336 ± 1 K (63 ± 1°C). Bottles were opened daily for 5 min, recapped and shaken end-over-end by hand for *ca*. 15 s.

Amorphous materials were removed from the samples in a 2 h treatment with 3 M H_2SO_4 at 323 K (50°C; Gasser *et al*., 1996). Similar treatments were used by Schwertmann and co-workers to purify synthetic goethites substituted with Cr and V (Schwertmann *et al*., 1989; Schwertmann & Pfab, 1994). Samples were washed four times with distilled water prior to oven drying at 323 K (50°C) overnight. After drying, the samples were crushed gently in an agate mortar. Reagent grade chemicals only (Prolabo, Normapur), were used for this study.

Total metal concentrations

Total metal concentrations and the corresponding X_{Mn} of the goethite samples were determined in duplicate by total dissolution. A 33 mg sample of goethite was placed in a Teflon container, 5 ml nitric acid (65% w/w) was added and the container was placed in a microwave oven for 30 min. The completely dissolved sample was then transferred to a 100 ml volumetric flask and brought to volume with distilled water. The Mn and Fe concentrations were determined by inductively coupled plasma atomic emission spectroscopy (ICP-AES; Jobin Yvon J38S). The relative error of the duplicates was <0.009; on average, 0.003.

Mineralogy

Bulk sample mineralogy was determined on powder mounts by X-ray diffraction (XRD) on a

100 mg goethite sample mixed with 100 mg $Pb(NO_3)_2$ as an internal standard. A DIANO 8000 diffractometer with a refracted beam graphite monochromator and Cu-$K\alpha$ radiation was used to produce step scans between 17 and 66°2θ with a step size of 0.02°2θ at a counting time of 6 s per step. Ten XRD lines (110, 120, 130, 021, 040, 111, 140, 221, 240 and 160) with a relative intensity of $I \geqslant 0.08$ were used to calculate the unit-cell dimensions of the samples. Both XRD line positions and unit-cell dimensions *a, b, c* and *v* were calculated with a tan θ weighting scheme as indicated earlier (Schwertmann *et al*., 1989). The presence of magnetic cubic phases was checked by measuring magnetic susceptibility (MS) using an Agico (Brno, Czech Republic) KLY-2 instrument.

Transmission electron microscopy

Five goethite samples with X_{Mn} = 0.025, 0.050, 0.077, 0.099 and 0.125 mol mol^{-1} (Table 1) were selected for transmission electron microscopy (TEM) investigation to obtain a subseries of samples that was evenly spaced in X_{Mn}. Preliminary experiments had revealed that a HCl treatment after removal of amorphous material helped to resuspend the goethites. For grid preparation, 25 mg goethite were placed in an acid-washed 50 ml Oak Ridge centrifuge tube filled with 30 ml of 1 M HCl. After shaking end-over-end at 3 revolutions per min for 1 h, the samples were centrifuged, washed twice with distilled water and resuspended in 30 ml water (16 MΩ). One ml of this suspension was diluted with distilled water in a 50 ml volumetric flask and sonicated for 10 min. A small quantity was pipetted onto a lacey carbon formvar-coated 150 mesh hexagonal copper grid (Ted Pella Inc., Redding, CA, USA). The TEM pictures and electron diffraction (ED) patterns were obtained on a JEOL 200CX TEM/STEM analytical electron microscope (NCEM, 1993). While TEM provided information about shape and size of the crystals, ED allowed verification of the needle mineralogy. The AEM was operated with an LaB_6 filament at 200 kV (see Krishnan & Echer, 1987).

Energy dispersive analysis of X-rays

The EDAX was performed on the same grids and simultaneously with TEM and ED. The AEM was equipped with a KEVEX 8000 microanalytical system and attached to a DEC LSI 11/73 computer. Iron and Mn concentrations were determined from three spot readings (core and each tip) on three visually (TEM) isolated needles per sample using an average beam diameter of 30 nm. The maximum thickness of the excited sample volume was >100 nm (Williams & Carter, 1996), i.e. EDAX was assessing the whole depth of the sample. Metal concentrations were determined using both Fe- and Mn-$K\alpha$ radiation and K factors of 1.0000 and 0.9703, respectively (Krishnan & Echer, 1987). Metal concentrations were also obtained by rastered beam analysis of an area of 2.5×2.5 μm^2. For one sample, line profiles (NCEM, 1993) with 10 points each were obtained of two isolated needles (parallel to the crystallographic *c* direction). The EDAX

TABLE 1. Mn mole fraction X_{Mn} [mol mol^{-1}] for selected samples as determined by total dissolution and spot EDAX analyses. Average values of EDAX spot analyses followed by the same letter are not significantly different ($p<0.05$). The total number of spot EDAX analyses was n = 44 (M3, M4, M6 and M8: n = 9 each, M5: n = 8). Generally, EDAX spot analyses were obtained from the two tips and the core of the studied needles.

Sample	Mn mole fraction X_{Mn}				
	Added (reactant solution)	Dissol. (goethite)	EDAX spot analysis Average	SD	CV
M3	0.025	0.025	0.027 a	0.017	0.63
M4	0.050	0.050	0.043 ab	0.024	0.55
M5	0.075	0.077	0.065 bc	0.018	0.28
M6	0.100	0.099	0.088 c	0.022	0.25
M8	0.125	0.125	0.163 d	0.039	0.23

SD: standard deviation; CV: coefficient of variation.

results are based on analyses of $>10^5$ counts.

Calculations

The terms 'significant' or 'significantly' are used if p was <0.05 to reject the null hypothesis. Linear regression results are generally reported as follows: $y = m(SE_m)x + b(SE_b)$; r^2 (starred, depending on the level of the probability p: *: <0.05, **: <0.01 and ***: <0.001), where y is the dependent and x the independent variable, m is the slope, b the intercept and r^2 the coefficient of determination of the regression equation, and, finally, SE_m and SE_b are the standard errors of m and b, respectively. Student's t was used to test both the difference between two means and between two linear regression slopes (Steel and Torrie, 1980). The sign test was performed following the method used by O'Mahony (1986).

RESULTS

The sole phase detected by XRD in powder mounts of the samples was goethite. There were highly significant linear correlations ($0.938*** \leqslant r^2 \leqslant 0.973***$, $n = 8$) between the unit-cell parameters *a, b, c* and *v* and X_{Mn} [mol mol^{-1}]: a[nm] = $-0.0166(11) \times X_{Mn} + 0.46177(9)$, b[nm] = $0.0264(21) \times X_{Mn} + 0.99553(17)$, c[nm] = $-0.0100(10) \times X_{Mn} + 0.30240(8)$, and v[nm^3] = $-0.0059(6) \times X_{Mn} + 0.13902(5)$. There was also a highly significant linear correlation with a slope of 1 and zero intercept between the ratio of Mn/Fe in goethite (R_{Gt}) *vs*. Mn/Fe in the initial solutions (R_i): $R_{Gt} = 0.986(13) \times R_i + 0.001(1)$ with $r^2 \leqslant 0.999***$ and $n = 7$. The MS of samples M1 to M8 was $331 \pm 13 \times 10^{-9}$ m^3 kg^{-1}. Linear regression showed that the correlation between MS and X_{Mn} was not significant and the slope was not different from zero.

The TEM pictures revealed that all the samples were needle shaped. Needles were generally present with their crystallographic *c* axis parallel to the plane of the grid (Fig. 1). Most commonly, particles were between 500 and 2500 nm long and 80 to 120 nm wide.

The total dissolution data showed that the Mn mole fraction X_{Mn} was $\leqslant 0.125$ mol mol^{-1} (Table 1). There was a significant linear correlation for X_{Mn} between rastered EDAX analysis and total dissolution ($n = 5$, $r^2 = 0.986***$; Fig. 2a). Neither the slope of this regression was significantly different from one, nor was the intercept significantly different from zero. Similar results were obtained for a linear regression of X_{Mn} between spot EDAX analysis and dissolution ($n = 5$, $r^2 = 0.889*$; Fig. 2b).

Not discriminating between tip and core, the spot EDAX analysis showed a considerable (within sample) variation of X_{Mn} among individual needles of a given sample (Table 1; Fig. 2b). The average standard deviation of X_{Mn} was 0.024 mol mol^{-1} (Table 1). With increasing X_{Mn}, the coefficient of variation decreased from 0.63 (M3) to 0.23 (M8; Table 1).

The X_{Mn} of cores and tips in 15 needle specimens out of five Mn-goethite samples are shown in Table 2. For a given sample (e.g. M3), the X_{Mn} value was generally significantly greater in cores as compared to tips. A sign test for all investigated needles also showed that the cores are significantly higher in X_{Mn} than the tips ($p = 0.001$; Table 2). This finding was supported by line scans performed on two additional needles (M6.4 and M6.5) of sample M6 (Fig. 3), where the X_{Mn} values ranged from 0.07 to 0.12 for needle M6.4 and from 0.08 to 0.11 for needle M6.5. The slopes of the two linear regressions of X_{Mn} (spot EDAX analyses) *vs*. distance were significantly different ($p<0.001$).

DISCUSSION

Mineralogy

The strong linear correlation between the unit-cell parameters (*a, b, c* and *v*, as calculated from XRD results) and X_{Mn} supported the incorporation of Mn into the structure of goethite. The sign and values of the regression slopes m_i (i = *a* through *c*) favoured a high-spin Mn^{3+} incorporation (Stiers & Schwertmann, 1985). The opposite signs of m_i (for i = *a*, *c*: sign '−'; b: '+') were caused by a distortion of the MnO_6^{9-} group (Mn^{3+}: Jahn-Teller effect; Sherman, 1984). In agreement with XRD results, neither the ED patterns nor MS suggested the presence of a phase other than goethite (e.g. jacobsite). It is concluded that the investigated samples were pure goethite, i.e. single phases. The linear correlation between R_{Gt} and R_i were in line with the data of Lewis & Schwertmann (1979), who observed a similar trend between Al/Fe in Al-goethite *vs*. $Al/Fe(OH)_4^-$ in the initial ferrihydritic suspensions.

Goethite consisted of 'needles' only (Fig. 1), i.e.

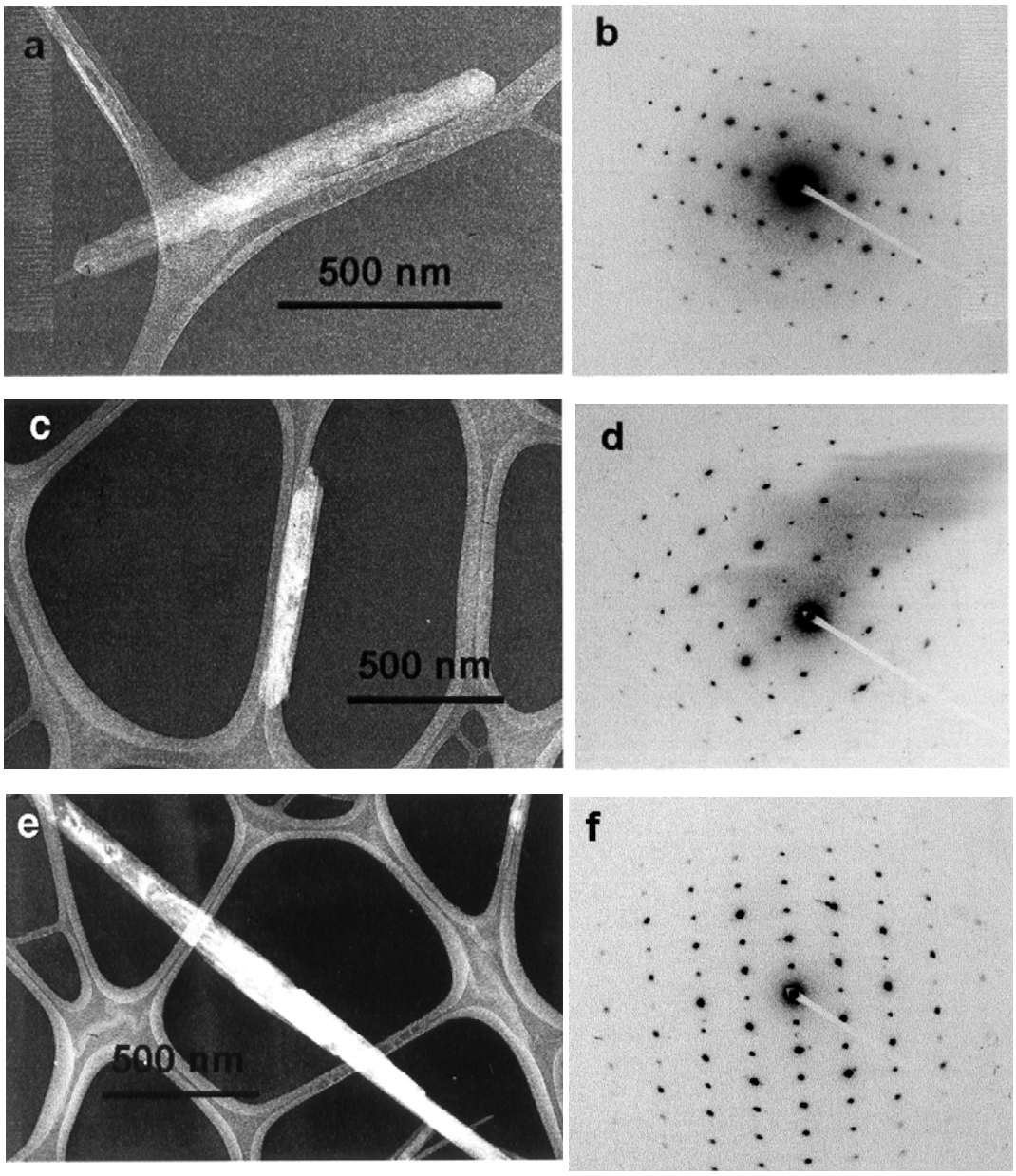

FIG. 1. Selected transmission electron micrographs (a, c and e) and electron diffraction patterns (b and f [100] zone, and d [210] zone) of three individual needles, from top to bottom: sample M3, M4 and M8 with X_{Mn} = 0.025, 0.050 and 0.125 [mol mol^{-1}], respectively.

it was present in the acicular form which is the principal habit of goethite (Cornell & Schwertmann, 1996). Based on a very low metal concentration in alkaline solutions (pH 12; <0.2 μM Fe and Mn, i.e. <0.02% of total metal), Giovanoli & Cornell (1992) stated that during 'Mn with Fe' coprecipitation, both metals were instantaneously and completely incorporated into Mn-ferrihydrite. Also, upon its subsequent transformation into goethite, no Mn was detected in solution (Cornell & Giovanoli, 1987).

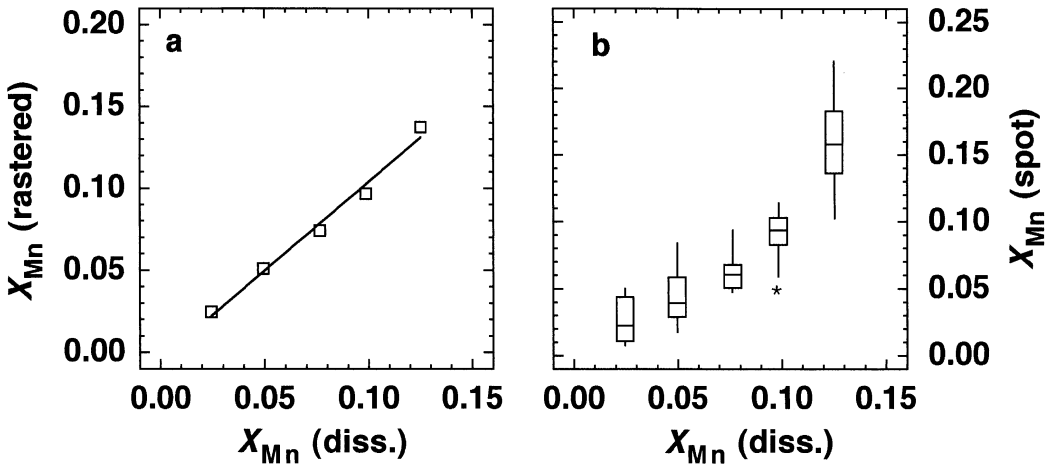

FIG. 2. (a) Mn mole fraction X_{Mn} [mol mol^{-1}] as seen from rastered EDAX *vs*. total dissolution analyses. The rastered area was 2.5×2.5 μm^2; regression parameters: $y = 1.082(73) \times x - 0.004(6)$; $r^2 = 0.986$***, $n = 5$. (b) Box plots of X_{Mn} [mol mol^{-1}] from EDAX spot *vs*. total dissolution analyses. The beam diameter was 30 nm; regression parameters: $y = 1.27(26) \times x - 0.020(26)$; $r^2 = 0.889$*, $n = 5$.

The cited work by Cornell & Giovanoli suggests that in the present study no significant amount of Mn was lost from the present system before the H_2SO_4 treatment. The spot EDAX analyses revealed that on the scale of the spot beam diameter (30 nm), no clusters of Mn were detectable, indicating the absence of any pure Mn compounds; this finding is in line with the mineralogical results discussed above.

Nevertheless, there was considerable within-sample (e.g. M3) variation of X_{Mn} as seen from the coefficients of variation ($0.23 \leqslant CV_x \leqslant 0.63$; see Table 1, Fig. 2b). The variation was partly attributed to the fact that the needle tips generally had a significantly lower X_{Mn} than the cores (Table 2). This finding was supported by the line scans (Fig. 3). Because Mn-goethites dissolve congruently in strongly acidic media (Lim-Nunez & Gilkes, 1987), a preferential dissolution of Mn during the H_2SO_4 treatment, which could also lead to such variation in X_{Mn}, seems unlikely. The higher X_{Mn} in needle cores as compared to tips (Table 2) and the linear relation between X_{Mn} and distance (Fig. 3) suggested Mn zoning in the studied goethites.

One reason for this suggested zoning may be the conditions of goethite crystal growth as reported for a similar synthesis by Cornell & Giovanoli (1987). Although incorporation of Fe and Mn upon transformation of ferrihydrite into goethite was congruent over the bulk of the reaction, Mn was incorporated less readily at the beginning of the transformation (Cornell & Giovanoli, 1987): "This initial discrepancy arose because Mn released by dissolution of ferrihydrite before goethite had nucleated, readsorbed onto the remaining ferrihydrite". In such a way, Mn zoning in ferrihydrite may lead to transformation-induced Mn zoning in goethite. Because of the similarity of the synthesis, the above mentioned obervations by Cornell & Giovanoli (1987) are likely to apply to this study as well. In addition, neither temperature, pressure nor saturation, which are common reasons for chemical zoning, can explain the variation of X_{Mn} within the needles.

Another reason for the suggested Mn zoning may be the oxidation of Mn(II) to Mn(III). Calculations were carried out based on the Mn added initially, in this study. The results suggested that enough dissolved O_2 to oxidize all the Mn in the sample before uncapping the first time was only present in samples M2 to M4. Samples M3 and M4, however, showed the within-sample variation as well (Table 1: CV = 0.63 and 0.55, respectively), indicating that total dissolved O_2 is unlikely to be the most important factor for Mn zoning in goethite.

The EDAX spot analyses also suggested an important variation of core X_{Mn} within a given

TABLE 2. Comparison of Mn mole fraction X_{Mn} [mol mol^{-1}] in cores and tips (tips, average of two measurements) of goethite needles. The t-test was calculated to compare the means of needle cores and tips within one sample (e.g. M3). The sign is positive if for a given needle the X_{Mn} is greater in the core than in the tip; the total number of comparisons was 15 with 14 '+' signs and one '−' sign (p<0.001).

Sample (X_{Mn} in goethite)	Needle	X_{Mn}		t-test	Sign
		Core	Tip		
M3	1	0.022	0.012		+
	2	0.044	0.049		–
(0.025)	3	0.036	0.011		+
	Mean (SD)	0.034(11)	0.024(22)	0.180	
M4	1	0.039	0.030		+
	2	0.074	0.062		+
(0.050)	3	0.058	0.018		+
	Mean (SD)	0.057(18)	0.036(23)	0.090	
M5	1	0.068	0.048		+
	2	0.093	0.060		+
(0.077)	3	0.091	0.054		+
	Mean (SD)	0.084(14)	0.054(6)	0.013	
M6	1	0.103	0.077		+
	2	0.088	0.071		+
(0.099)	3	0.111	0.098		+
	Mean (SD)	0.101(12)	0.082(14)	0.020	
M8	1	0.177	0.147		+
	2	0.143	0.103		+
(0.125)	3	0.214	0.183		+
	Mean (SD)	0.178(35)	0.144(40)	0.005	

SD: standard deviation.

sample (Table 2; $0.12 \leqslant CV \leqslant 0.33$). Since cores contained the seeds (oldest parts of the needles), this variation argued in favour of goethite seeds that differ in X_{Mn} values. If all the needle cores were of the same age, the different slopes of needle M6.4 and M6.5 might indicate an individual crystal growth in terms of X_{Mn}. The latter two points need additional attention in future research.

It may be speculated that zoning in Mn-substituted goethite may affect diagnostic XRD peaks, infrared bands, the thermal transformation of goethite to hematite, chemical reactivity (e.g. adsorption/desorption and dissolution) and other properties. Because of the data obtained in this study, the following paragraph is restricted to XRD only.

The question was whether the variation of X_{Mn} contributed to the broadening of XRD peaks. The XRD peak positions of an Fe oxide (e.g. goethite) are dependent on its degree of substitution with another cation, i.e. chemical variation between samples (Cornell & Schwertmann, 1996, and references therein). The influence of substitution is generally more pronounced at higher angles (2θ). For instance, the expected positions of two (supposed) Mn-goethites of the present series M (X_{Mn} = 0.12 and 0.20, respectively; Cu-$K\alpha$ radiation) were 63.90 and 63.83°2θ, respectively for hkl = 061. Also, because in the present study a considerable variation of X_{Mn} within a given sample was observed, XRD peak broadening may not be excluded *a priori*. A Rietveld calculation indicated that resulting peaks were symmetrical (H. Stanjek, pers. comm.). Because the X_{Mn} values mentioned

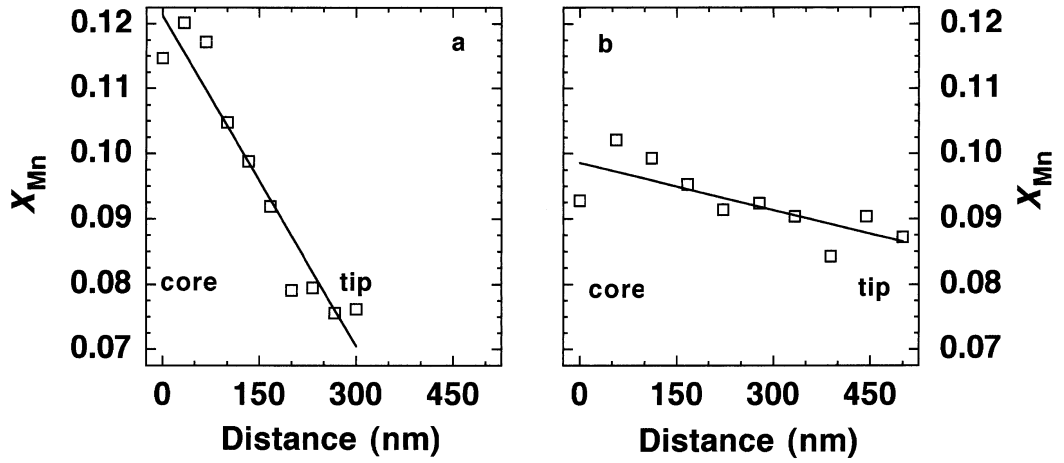

FIG. 3. Distribution of Mn mole fraction X_{Mn} [mol mol^{-1}] (spot EDAX: beam diameter = 30 nm) *vs*. distance *d* (nm) between core and one tip of two individual needles (M6.4 and M6.5). $y = -1.69(18) \times 10^{-4} \times x$ [nm] + 0.121(3), $r^2 = 0.921$***, $n = 10$; $y = -2.40(72) \times 10^{-5} \times x$ [nm] + 0.099(2), $r^2 = 0.585$**, $n = 10$. The slopes of the two regressions are significantly different ($p<0.001$).

before were in the range of the within-sample variation of sample M8 (Table 1), it was concluded that peak broadening due to this source of variation was generally $\ll 0.07°2\theta$, given the experimental conditions of this study. This result suggests, however, that this type of peak broadening is experimentally difficult to detect.

In the field of zoning, the present study brings forward some new evidence with data that argue in favour of Mn zoning in synthetic Mn-substituted goethite. Thus, the reported data may serve to prompt initial discussion, with further work to follow.

ACKNOWLEDGMENTS

This paper benefited from the analytical skills of Chuck Echer, the National Center of Electron Microscopy at Berkeley (CA, USA). The authors acknowledge analytical and instrumental support by H.V. Clausnitzer, W.A. Hobson, R.J. Southard, K.L. Verosub and R.J. Zasoski, all of the University of California at Davis (USA), as well as by G. Belgy of 'Centre de Pédologie Biologique' at Vandœuvre-lès-Nancy (France). Special thanks go to A. Hirt and R. Wessicken, ETH at Zurich, for their help with the interpretation of the MS data and ED patterns, respectively. The authors also acknowledge the stimulating comments by R. Giovanoli, U. Schwertmann, H. Stanjek and an anonymous reviewer. During the initial period of this research one of the authors (UGG) was supported by CNRS (France; URSSAF No. 540 547 171 861 and CIES grant No. 156249E).

REFERENCES

Bloss D.F. (1971) *Crystallography and Crystal Chemistry*. Holt, Rinehart & Winston, Inc. New York.

Cornell R.M & Giovanoli R. (1987) Effect of manganese on the transformation of ferrihydrite into goethite in alkaline media. *Clays Clay Miner.* **35**, 11–20.

Cornell R.M. & Schwertmann U. (1996) *Iron Oxides*. VCH, Weinheim.

Ebinger M.H. & Schulze D.G. (1989) Mn-substituted goethite and Fe-substituted groutite synthesized at acid pH. *Clays Clay Miner.* **37**, 151–156.

Ebinger M.H. & Schulze D.G. (1990) The influence of pH on the synthesis of mixed Fe-Mn oxide minerals. *Clay Miner.* **25**, 507–518.

Gasser U.G., Jeanroy E., Mustin C., Barres O., Nüesch R., Berthelin J. & Herbillon A.J. (1996) Properties of synthetic goethites with Co for Fe substitution. *Clay Miner.* **31**, 465–476.

Gerth J. (1990) Unit cell dimensions of pure and trace metal-associated goethites. *Geochim. Cosmochim. Acta*, **54**, 363–371.

Gharibi E., Jeannot F., Dupré B. & Gleitzer C. (1990) Influence of aluminium on the reduction of hematite into magnetite. Kinetic and morphological study. *Rev. Métall.: Mém. Etudes Scientif.* **87**, 86–91.

Giovanoli R. & Cornell R.M. (1992) Crystallization of

metal substituted ferrihydrites. *Z. Pflanzenernähr. Bodenk.* **155**, 455–460.

Junta J.L. & Hochella M.F. (1994) Manganese(II) oxidation at mineral surfaces: a microscopic and spetroscopic study. *Geochim. Cosmochim. Acta*, **58,** 4985–4999.

Krishnan K.M. & Echer C.J. (1987) Determination of UTW K_{XSi} factors for low-atomic-number micro-analysis: a systematic approach. Pp. 99–102 in: *Analytical Electron Microscopy — 1987* (D.C. Joy, editor). San Francisco Press, CA.

Lewis D.G. & Schwertmann U. (1979) The influence of aluminum on the formation of iron oxides. IV. The influence of [Al], [OH], and temperature. *Clays Clay Miner.* **27**, 195–200.

Lim-Nunez R. & Gilkes R.J. (1987) Acid dissolution of synthetic metal containing goethites and hematites. *Proc. Int. Clay Conf., Denver,* 197–204. (L.G. Schultz *et al*., editors).

NCEM (1993) *NCEM users' guide*. National Center for Electron Microscopy, Lawrence Berkeley Laboratory, Berkeley, CA.

O'Mahony M. (1986) *Sensory Evaluation of Food*. Marcel Dekker, New York.

Rösler H.J. (1983) *Lehrbuch der Mineralogie*. VEB Grundstoffindustrie. Leipzig.

Schwertmann U. (1984) The double dehydroxylation peak of goethite. *Thermochim. Acta*, **78**, 39–46.

Schwertmann U. & Cornell R.M. (1991) *Iron Oxides in the Laboratory*. VCH, Weinheim.

Schwertmann U. & Pfab G. (1994) Structural vanadium in synthetic goethites. *Geochim. Cosmochim. Acta*, **58**, 4349–4352.

Schwertmann U. & Taylor R.M. (1989) Iron oxides. Pp. 380–438 in: *Minerals in Soil Environments* (J.B. Dixon & S.B. Weed, Editors). Soil Sci. Soc. Am., Madison, WI.

Schwertmann U., Gasser U. & Sticher H. (1989) Chromium-for-iron substitution in synthetic goethites. *Geochim. Cosmochim. Acta*, **53**, 1293–1297.

Schulze D.G. (1982) *The identification of iron oxides by differential X-ray diffraction and the influence of aluminum substitution on the structure of goethite*. PhD thesis, Tech. Univ. München, Germany.

Shannon R.D. (1976) Revised effective ionic radii and systematic studies of interatomic distances in halides and chalcogenides. *Acta Crystallogr.* **A32**, 751–767.

Sherman D.M. (1984) The electronic structure of manganese oxide minerals. *Am. Miner.* **69**, 788–799.

Steel R.G.D. & Torrie J.H. (1980) *Principles and Procedures of Statistics*. McGraw-Hill, New York.

Stiers W. & Schwertmann U. (1985) Evidence for manganese substitution in synthetic goethite. *Geochim. Cosmochim. Acta*, **49**, 1909–1911.

Torrent J., Schwertmann U. & Barron V. (1987) The reductive dissolution of synthetic goethite and hematite in dithionite. *Clay Miner.* **22**, 329–337.

Vempati R.K., Morris R.V., Lauer H.V.J. & Helmke P.A. (1995) Reflectivity and other physicochemical properties of Mn-substituted goethites and hematites. *J. Geophy. Res.* **100E2**, 3285–3295.

Williams D.B. & Carter C.B. (1996) *Transmission Electron Microscopy*. Plenum Press, New York.

Zoltai T. & Stout J.H. (1984) *Mineralogy: Concepts and Principles*. Burgess Publ. Company, Minneapolis, MN.